Supplementary Data

Supplementary FIGURE LEGENDS

Supplementary Fig. 1 SL diet-induced β cell loss, ER stress and apoptosis in *Gck*$^{+/-}$ mice.
(A) Pancreatic sections were stained with antibodies to insulin (green) and glucagon (red). The scale bar represents 50 μm. (B) Pancreatic sections were stained with an antibody to CHOP. Arrows point to CHOP-positive cells. (C) Pancreatic sections were subjected to a TUNEL assay. Insulin is stained green, and TUNEL-positive nuclei are stained red. Arrows point to apoptotic nuclei. (D) Pancreatic sections were stained with antibodies to Ki67 (green) and insulin (red). Arrows point to proliferating cells. (E) Pancreatic sections were stained with antibodies to insulin (blue) and glucagon (red) (left panel), and to E-cadherin (green) (center panel). The merged images are also shown (right panel). The experiments were performed in *WT* and *Gck*$^{+/-}$ mice after the mice had been fed either the SO diet or the SL diet for 25 weeks.

Supplementary Fig. 2 DFS improved islet morphology, β cell mass, ER stress, and apoptosis in *Gck*$^{+/-}$ mice fed the SL diet.
(A) Pancreatic sections were stained with antibodies to insulin (green) and glucagon (red). The scale bar represents 50 μm. (B) Pancreatic sections were stained with an antibody to CHOP. Arrows point to CHOP-positive cells. (C) Pancreatic sections were subjected to a TUNEL assay. Insulin is stained green, and TUNEL-positive nuclei are stained red. Arrows point to apoptotic nuclei. (D) Pancreatic sections were stained with antibodies to Ki67 (green) and insulin (red). Arrows point to proliferating cells. (E) Pancreatic sections were stained with antibodies to insulin (blue) and glucagon (red) (left panel), and to E-cadherin (green) (center panel). The merged images are also shown (right panel). The experiments were performed in *WT* mice and *Gck*$^{+/-}$ mice after the mice had been fed either the SL diet or the SL diet plus DFS.

Supplementary Fig. 3 The SL diet increased arachidonic acid content in liver in both *WT* and *Gck*$^{+/-}$ mice.
The fatty acid content in liver from *WT* mice (A) or *Gck*$^{+/-}$ mice (B) were analyzed as described in Experimental Procedures (n = 4). The experiments were performed in *WT* mice and *Gck*$^{+/-}$ mice after 5 weeks on the SO diet, the SL diet, or the SL plus DFS diet. White bars, SO; black bars, SL; left hatched bars, SL + DFS. $*p < 0.05$.

Supplementary Fig. 4 Changes in blood glucose, insulin, and active GLP-1 concentrations in *WT* mice and *Gck*$^{+/-}$ mice during an oral meal tolerance test performed after feeding the mice the SO or SL diet for 20 weeks.

(A) Blood glucose, (B) serum insulin, and (C) serum active GLP-1 concentration at 0 min (fasted >20 h) and 30 min after the oral administration of an SO diet or an SL diet test meal (12 mg/g body weight) to 28-week-old *WT* mice and *Gck*$^{+/-}$ mice that had been fed either the SO or SL diet for 20 weeks (n = 3-4). To obtain a sufficient amount of whole blood to measure the biologically active form of GLP-1, blood was collected from the inferior vena cava under anesthesia with a DPP-4 inhibitor (Millipore) at the time points indicated. Blood glucose and serum insulin levels were determined using these samples.

Supplementary Fig. 5 Impact of exendin-4 on glucose-stimulated insulin secretion by the islets of *WT* mice and *Gck*$^{+/-}$ mice.

Insulin secretion by the islets of 12 – 14-week-old standard-chow diet-fed *WT* or *Gck*$^{+/-}$ mice in response to 2.8 mM, 8.3 mM or 22.2 mM glucose in the presence or absence of 100 nM exendin-4. The experiments were carried out according to two protocols: (A) immediately after islet isolation, and (B) after 12 hr of culture in a medium containing 11 mM glucose after islet isolation. The results are shown as nanograms insulin/10 islets/90 min (n=9). ∗: $P < 0.05$. Black bars, vehicle alone; gray bars, exendin-4. Of note, insulin secretion in response to glucose was impaired in the *Gck*$^{+/-}$ islets, but the fold-responses to glucose were larger in protocol (A) than in protocol (B), while the responses to exendin-4 were larger in protocol (B) than in protocol (A).

Supplementary Fig. 6 Effects of exendin-4 on apoptosis induced by a combination of high glucose and linoleic acid in MIN6 cells.

(A) Representative images of propidium iodide (PI)-stained nuclei and DAPI-stained nuclei in MIN6 cells treated with vehicle alone (ctl) and with 0.5 mM OA or LA in 25 mM glucose for 24 h, in the absence or presence of 50 nM exendin-4 (Ex-4). (B) Representative images of a flow cytometry analysis of Annexin V-FITC-stained MIN6 cells treated with vehicle alone (ctl) or the 0.5 mM OA or LA in 25 mM glucose for 24 h, in the absence or presence of 50 nM exendin-4 (Ex-4).

Supplementary Fig. 1

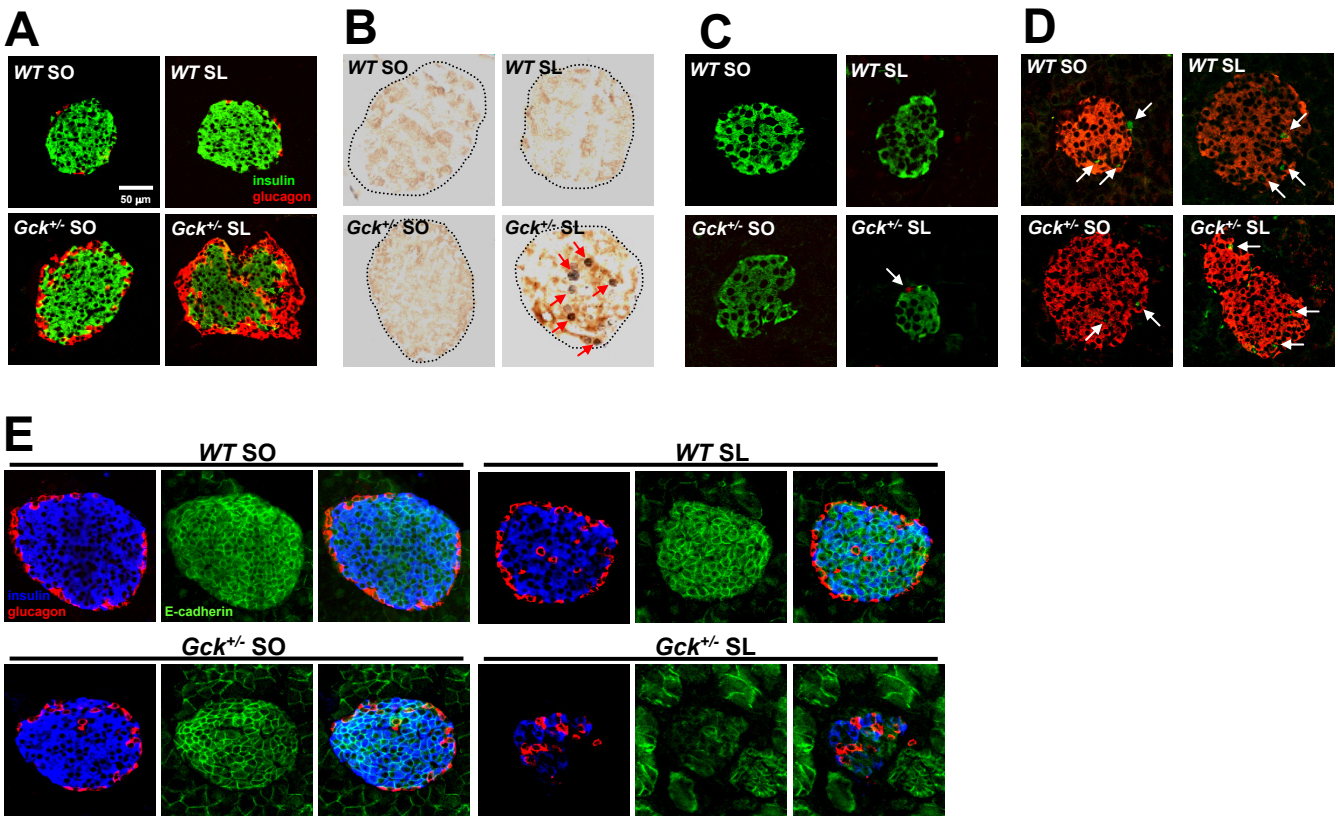

Supplementary Fig. 2

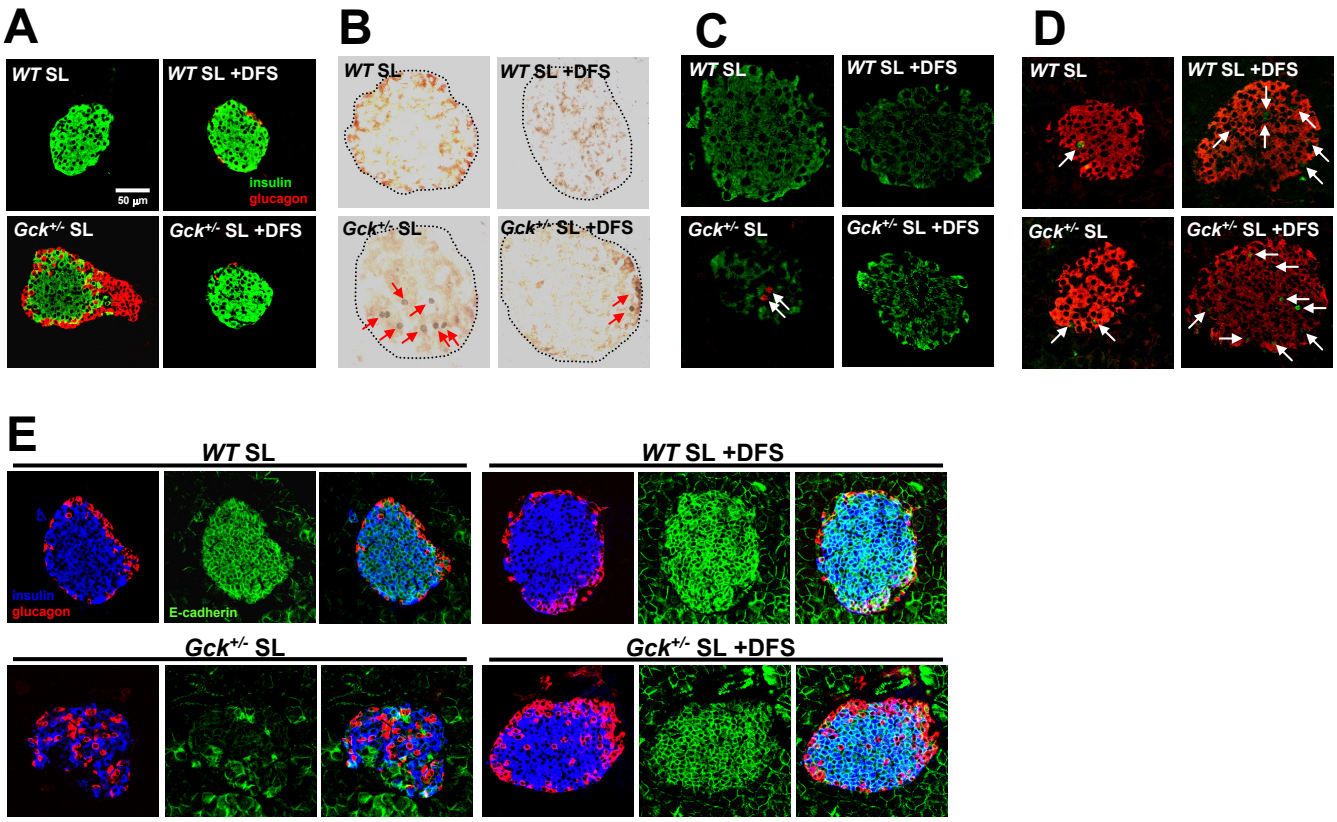

Supplementary Fig. 3

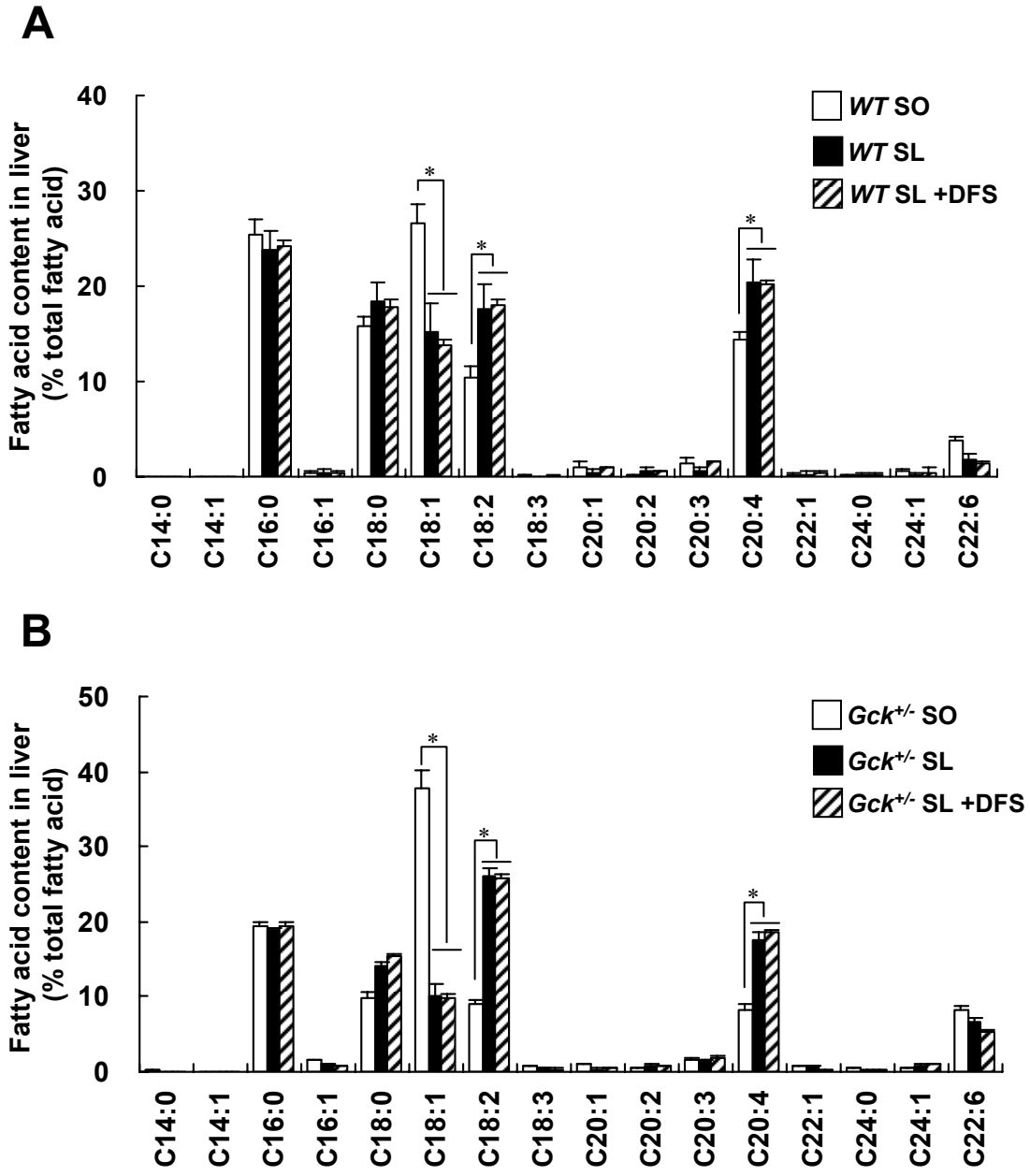

Supplementary Fig. 4

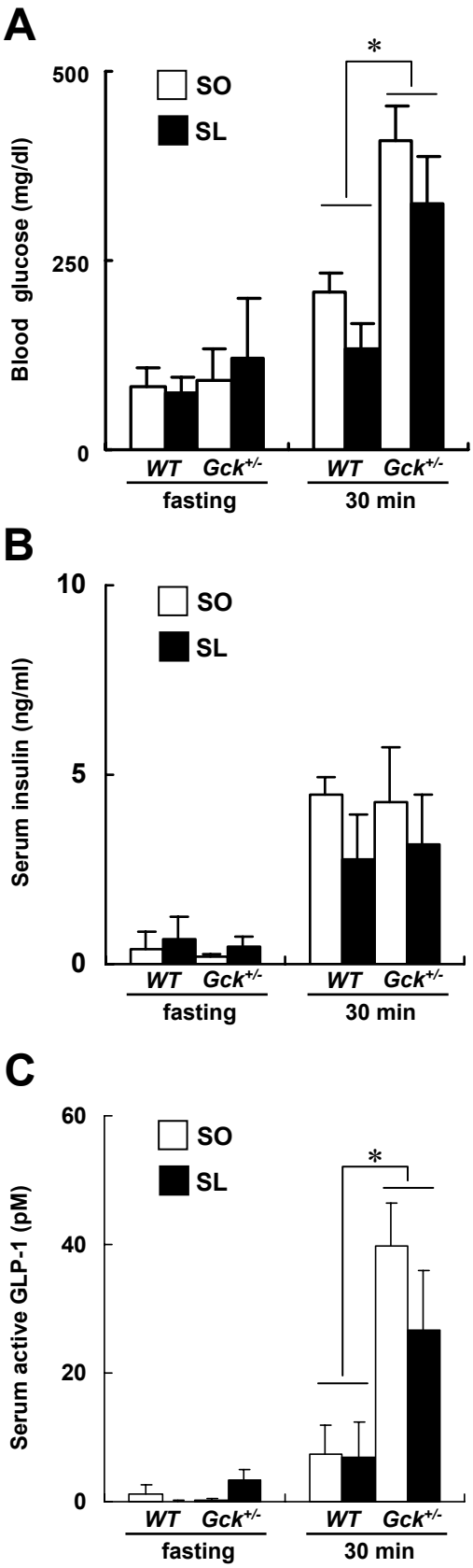

Supplementary Fig. 5

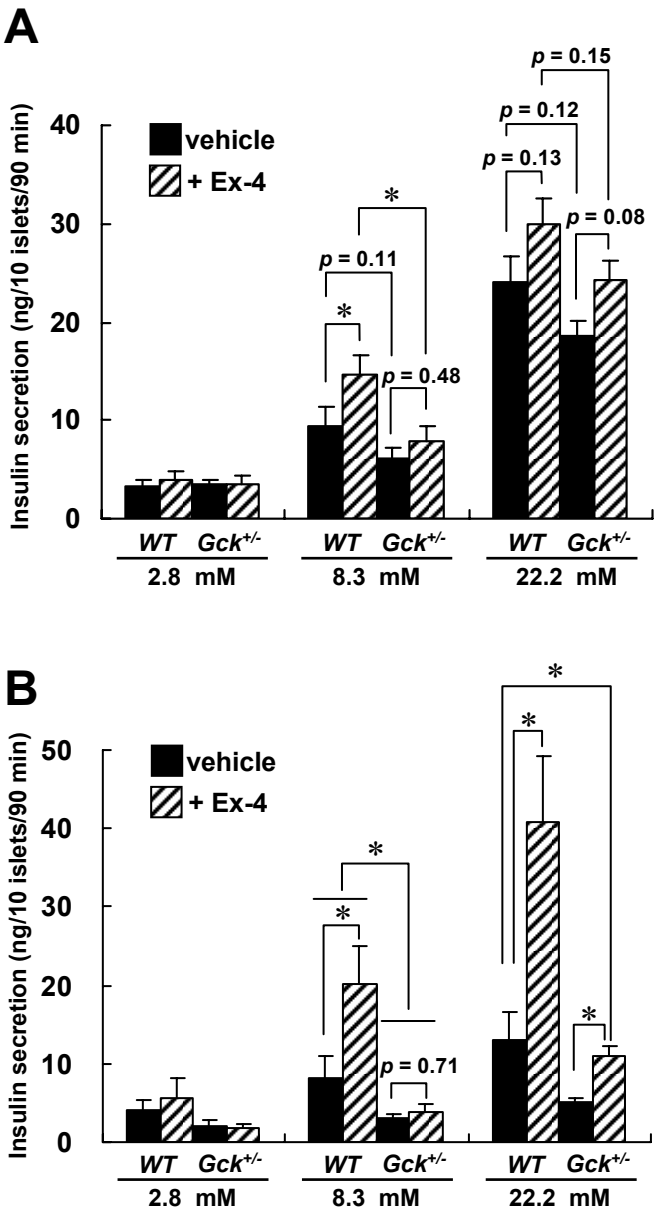

Supplementary Fig. 6